Comp. & Maths. with Appls. Vol. 12A, No. 6, pp. 777–784, 1986
Printed in Great Britain

0886–9553/86 $3.00 + .00
Pergamon Journals Ltd

IMAGE PLANE HOLOGRAPHY FOR HOLOGRAPHIC PRESENTATION OF A THREE-DIMENSIONAL DATA BASE

LAWRENCE HENDLER† and STEPHEN S. FRIEDLAND✠
School of Physics and Astronomy, Raymond and Beverly Sackler Faculty of Exact Sciences, Tel-Aviv University, Tel Aviv 69978, Israel

Abstract—Holographic presentation of three-dimensional data from CT, NMR, PET or ultrasonic scan should greatly aid in diagnostic and therapeutic procedures. Originally a multiplex white light hologram was formed from many X-rays of a cadaver's hand. Many methods of computer generating a hologram have been explored. In this paper we examine a method of calculating an Image Plane Hologram by computer and show the white light characteristics of the Image Plane Hologram.

INTRODUCTION

In previous works[1,2] various holographic techniques were discussed for CGH representation of the 3D data base produced in a CT, NMR, PET or ultrasonic scan. The holographic format has been demonstrated for presentation of X-ray data by means of a rainbow hologram[3]. The hand of a cadaver was photographed with X-rays in steps of one-third degree for a total of 1080 projections. From these frames a rainbow (white light) hologram was formed. Unfortunately, this method cannot be used in actual practice, but it does demonstrate the effectiveness of the holographic format. (This hologram can be viewed at the New York Museum of Holography.)

In converting three-dimensional data bases to holograms various approaches have been considered, including the method of Burch[4], the method of Lohmann and Brown[5], the method of Perlmutter and Friedland[1] for Fresnel Holograms, and currently we have started to consider generating Image Plane Holograms, which will be described in the article. Before discussing the details of the methods of generating a hologram, we will look at some general considerations.

Herbison–Evans[6] states that a typical hologram should have an area in the range of 10 cm^2. Fixed spacing should be approximately that of the wavelength of light, say, 5×10^{-5} cm; Therefore, the total number of pixels needed is $(2 \times 10^5)^2 = 4 \times 10^{10}$. For each pixel a real and imaginary part need be generated giving in the order of 10^{11} values. We must consider three problems:

(1) the time needed to calculate the values for the generation of the hologram,
(2) the amount of storage necessary,
(3) the time needed to reproduce the hologram.

1. *Calculation time*

The one-dimensional fast Fourier transform of n points requires $2n \log_2 n$ operations. For a two-dimensional $n \times n$ array of points $4n^2 \log_2 n$ operations are required. For $n = 2 \times 10^5$ pixels as indicated previously, the number of operations required is 3×10^{12}. If, for example, each operation requires 0.3 μs, then a total time of 10^6 s = 10 days would be required.

2. *Storage*

For disk units storing 1000-M bytes, 100 units are required to store the transformed image of 10^{11} values.

3. *Reproduction time*

In using a plotting routine on paper to be photographed and reduced and allowing approximately 1 s per point plotting time, then for 10^{11} points, 100 years plotting time is

†Present address: Optrotech Ltd, Industrial Zone B, POB 69, Nes Ziona 70450, Israel.
✠Professor Friedland passed away in May 1985.

required. With an oscilloscope plot at 10^6 points per second, plotting time is reduced, but only $10^3 \times 10^3$ resolvable points can be recorded requiring the hologram to be recorded in 40,000 parts.

On the other hand, a typical CT scan provides data for a 256×256 matrix or approximately 6×10^4 points compared to the previously stated 4×10^{10} points. This reduces the problem of calculation time, storage and reproduction time. However, if the pixels are spaced at the order of magnitude of the wavelength of light, the size of the hologram which will be produced is $256 \times 256 \times [5 \times 10^{-5}]^2\ \text{cm}^2 = 0.016\ \text{mm}^2$, which is not a very useful size for a hologram.

HOLOGRAM TYPES

There exist several methods of recording a hologram: the kinoform uses two layers of film. One layer records amplitude information by means of gray levels, and the other layer records phase information by varying film thickness. In the method developed by Lohmann and Brown[5] the quantity of light transmitted by a pixel on a film is proportional to the size of an opening in a pixel, while the phase is related to the position of the opening in the pixel. The Burch method will be elaborated on in the next section.

All of these techniques provide the means of encoding complex diffraction patterns into real value patterns that can be used to expose holographic films. There are various ways to choose the diffraction patterns.

1. *Fourier transform*

The far field, or Fraunhofer diffraction pattern, can be computed with a Fourier transform. This transform accurately describes the diffraction pattern when the image is an infinite distance from the film plane. The depth-dependence of the planes within the image is not preserved. In a hologram formed by the superposition of Fourier transforms of the original subject's various planes, the depth information will be lost.

2. *Fresnel transform*

Computing a Fresnel transform solves the problem of an image at infinity and prevents the loss of depth information. The traditional method of computing a Fresnel transform is based on the FFT. Unfortunately, an FFT program with a data base of $(2 \times 10^5)^2$ is beyond present-day capabilities of computers. It has been recognized that one can compute large-area Fresnel diffraction patterns based upon a multitude of two-dimensional FFTs. Each two-dimensional FFT is on the order of 256×256 in dimension, which is compatible with the cross-section of scan data.

3. *Multiplex hologram*

The projection of the object at a series of angles can be readily obtained from the stored three-dimensional array. Digital processing of these perspective views produce a multiplex hologram. Although this method does not give a true three-dimensional image, but rather an image by stereopsis, it does have the advantage that the hologram can be viewed in white light.

4. *Image plane holography*

Image plane holography[7–9] (IPH) provides a true three-dimensional image, like most other forms of holography, in the sense that different planes can be found in viewing the reconstructed image. IPH also enjoys the advantage of reconstruction in white light. Basically, they are Fresnel holograms made very close to the object. In most cases proximity is created by the use of lenses. This creates an extreme localization of the diffraction pattern in the recording medium.

Another common method for creating image plane holograms is by making a hologram of a hologram. By illuminating a hologram with the conjugate to the reference beam, a real image is created. Again, a hologram is made of the real image resulting in the localization of the diffraction pattern in the recording medium.

COMPUTATION OF THE IMAGE PLANE HOLOGRAM

The basic equation of the hologram recording method is the expression for the transmittance distribution $t(x_0, y_0)$ of a light modulating medium such as film

$$t(x_0, y_0) = |R(x_0, y_0)|^2 + |U(x_0, y_0)|^2 + 2\,\mathrm{Re}(R^*(x_0, y_0)U(x_0, y_0)). \tag{1}$$

$R(x_0, y_0)$ is a reference wave, $U(x_0, y_0)$ is the complex diffraction field of the source volume, and Re denotes the real part of the argument. The reference wave is an offset plane wave

$$R(x_0, y_0) = \exp\{i2\pi\beta y_0\}, \quad \beta = \sin \nu/\lambda, \tag{2}$$

where ν is the angle between the normal to the hologram and the Poynting vector of the plane wave.

Burch recognizes that the image information is contained in the third term of Eq. (1), whereas the self-interference term $|U(x_0, y_0)|^2$ is unimportant, since it does not contribute directly to image formation. If the self-interference term is not present, then ν, the offset angle, can be reduced, thereby reducing the band width requirements of the recording device.

The self-interference term cannot be avoided in optical holography, but in computer generated holography it can be ignored. Burch therefore suggests recording the transmittance function as

$$t(x_0, y_0) = R_0 + \mathrm{Re}(R^*(x_0, y_0)U(x_0, y_0)), \tag{3}$$

where R_0 is a bias guaranteeing that $t(x_0, y_0)$ is not negative.

To view the reconstructed image the hologram is illuminated by the offset plane wave $R(x_0, y_0)$, thereby recreating the virtual image wavefront. The aperture in the hologram plane will limit both the field of view and the image resolution. It is, therefore, desirable to produce the largest possible hologram.

THE IMAGE MODEL

We assume a three-dimensional array of monochromatic point sources. The amplitude and phase of each point source is proportional to the value of the corresponding datum. Furthermore, we assume that the data are organized into a sequence of k parallel two-dimensional cross-sections. We can define the source distribution $f(x, y; z)$ to be

$$f(x, y; z) = \sum_{n=0}^{k=1} \left(\sum_{j=0}^{n-1} \sum_{k=0}^{n-1} f_s(j, k; n)\delta(x - j\Delta_x, y - k\Delta_y, z - n\Delta_z) \right). \tag{4}$$

$\delta(\cdot,\cdot;\cdot)$ is the 3D Dirac delta function and Δ_x and Δ_y is the distance between points in the x and y directions.

$f_s(j, k, n)$ are complex values corresponding to complex source amplitude at the points $(j\Delta_x, k\Delta_y, n\Delta_z)$ in the (x, y) plane at the distance $z_0 + n\Delta_z$. The subscript s indicates that the function is defined at discrete points.

THE DIFFRACTION PATTERN

To calculate the two-dimensional complex field distribution in the hologram plane $F_\alpha(x_0, y_0)$ from $f(x, y)$, the two-dimensional complex source distribution, we apply the Huygen–Fresnel principle in terms of a superposition integral[10]

$$F_\alpha(x_0, y_0) = \int\int f(x, y)h(x_0, y_0; x, y)\,\mathrm{d}x\,\mathrm{d}y. \tag{5}$$

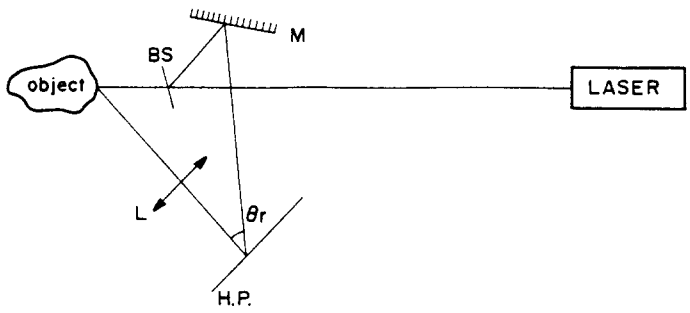

Fig. 1. An arrangement for IPH. M, mirror; BS, beam splitter; L, imaging lens; H.P., holographic plate.

Therefore, the problem amounts to finding the point spread function of the system we are using.

A typical geometry for IPH appears in Fig. 1, while the point spread function can be seen to derive from the imaging geometry, as shown in Fig. 2. The field distribution in the holographic plane x_0, y_0 is seen to derive from the field distribution after the lens in plane x_1, y_1 which itself derives from the free propagation of a point source and the transmittance function of the lens (being a phase shift),

$$f(x, y) = \frac{A \exp\{ikr_s\}}{r_s} T(x, y), \tag{6}$$

and for a lens of radius b and focal length f,

$$T(x, y) = \begin{cases} \exp\{-ik(x^2 + y^2)/2f\}, & x^2 + y^2 < b, \\ 0, & x^2 + y^2 > b. \end{cases} \tag{7}$$

Using the paraxial approximation and transferring to polar coordinates and using the relationship[11]

$$F(x_0, y_0, z_0) = \frac{2\pi}{i\lambda z_0} \exp(ikr_0) \int_0^b \rho T(\rho) \exp\{ik\rho^2/2z_0\} J_0\left(\frac{k\rho\rho_0}{z_0}\right) d\rho, \tag{8}$$

we see that

$$F(x_0, y_0, z_0) = \frac{2\pi}{i\lambda z_0 z_s} \exp(ikr_0) \exp(ikz_s) \int_0^b \rho \exp\left\{\frac{ik\rho^2}{2}\left(\frac{1}{z_s} + \frac{1}{z_0} - \frac{1}{f}\right)\right\} J_0\left(\frac{k\rho\rho_0}{z_0}\right) d\rho. \tag{9}$$

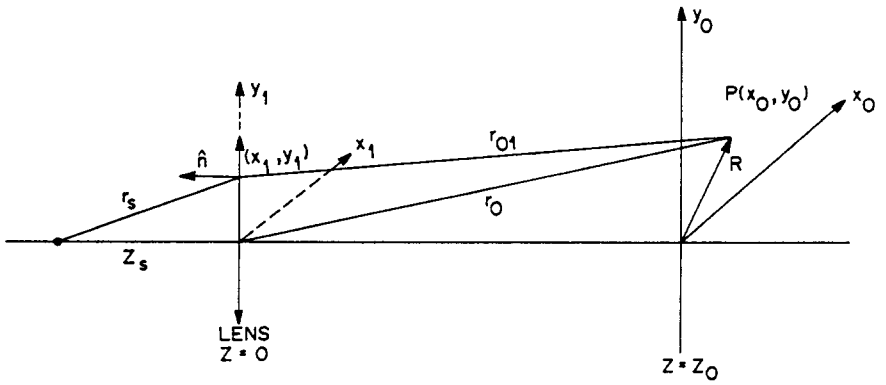

Fig. 2. Geometry for imaging a point source by a lens. Lens is located in plane x_1, y_1. Field distribution is examined in plane x_0, y_0 distance z_0 from lens.

The quality of the imaging is expressed by the terms

$$\frac{1}{z_s} + \frac{1}{z_0} - \frac{1}{F} = \frac{1}{\epsilon}. \tag{10}$$

Of course, if the point is well-imaged,

$$1/\epsilon = 0. \tag{11}$$

The integral

$$\int_0^b \rho \exp\left\{\frac{i}{2} m\rho^2\right\} J_0(n\rho)\, d\rho, \quad m = k/\epsilon, \quad n = k\rho_0/z_0 \tag{12}$$

must now be computed. Expressing

$$\exp\left\{\frac{i}{2} m\rho^2\right\} = \cos \tfrac{1}{2}m\rho^2 + i \sin \tfrac{1}{2}m\rho^2, \tag{13}$$

the integral becomes

$$2\int_0^b \rho J_0(n\rho) \cos(\tfrac{1}{2}m\rho^2)\, d\rho + 2i \int_0^b \rho J_0(n\rho) \sin(\tfrac{1}{2}m\rho^2)\, d\rho = C(n, m) + iS(n, m), \tag{14}$$

using the identity

$$\frac{d}{d\rho}[\rho^{n+1} J_{n+1}(\rho)] = \rho^{n+1} J_n(\rho), \tag{15}$$

and integrating by parts

$$C(n, m) = \frac{2}{n}\left[bJ_1(nb) \cos(\tfrac{1}{2}mb^2) + m\int_0^b \rho^2 J_1(n\rho) \sin(\tfrac{1}{2}m\rho^2)\, d\rho\right]. \tag{16}$$

Repeating the process, we find

$$\begin{aligned} C(n, m) = {} & \frac{\sin(\frac{1}{2}mb^2)}{\frac{1}{2}m} \sum_{q=0}^{\infty} (-1)^q \left(\frac{mb}{n}\right)^{2q+2} J_{2q+2}(nb) \\ & + \frac{\cos(\frac{1}{2}mb^2)}{\frac{1}{2}m} \sum_{q=0}^{\infty} (-1)^q \left(\frac{mb}{n}\right)^{2q+1} J_{2q+1}(nb). \end{aligned} \tag{17}$$

Defining the Lommel functions

$$\begin{aligned} U_1(u, v) &= U\int_0^1 \rho \cos\left[\frac{u}{2}(1 - \rho^2)\right] J_0(v\rho)\, d\rho, \\ U_2(u, v) &= U\int_0^1 \rho \sin\left[\frac{u}{2}(1 - \rho^2)\right] J_0(v\rho)\, d\rho, \end{aligned} \tag{18}$$

expanding the sine and cosine into the Taylor series, we obtain

$$\begin{aligned} U_1(u, v) &= \sum_{n=0}^{\infty} (-1)^n \left(\frac{u}{v}\right)^{2n+1} J_{2n+1}(v), \\ U_2(u, v) &= \sum_{n=0}^{\infty} (-1)^n \left(\frac{u}{v}\right)^{2n+2} J_{2n+2}(v), \end{aligned} \tag{19}$$

giving

$$C(n, m) = \frac{\sin(\frac{1}{2}mb^2)}{\frac{1}{2}m} U_2(mb^2, nb) + \frac{\cos(\frac{1}{2}mb^2)}{\frac{1}{2}m} U_1(mb^2, nb). \tag{20}$$

Solving in a similar fashion for $S(n, m)$

$$S(n, m) = \frac{\sin(\frac{1}{2}mb^2)}{\frac{1}{2}m} U_1(mb^2, nb) + \frac{\cos(\frac{1}{2}mb^2)}{\frac{1}{2}m} U_2(mb^2, nb). \tag{21}$$

We can now substitute and find the field distribution for a point source imaged by a lens, which is the point spread function $h(x_0, y_0, x, y)$ in Eq. (5).

$$\begin{aligned} h(x_0, y_0; x, y) &= F(x_0, y_0, z_0) \\ &= \frac{\pi A}{i\lambda z_0 z_s} \exp(ikr_0) \exp(ikz_s) \left\{ \frac{2}{m} [\sin(\tfrac{1}{2}mb^2) U_2(mb^2, nb) \right. \\ &\quad + \cos(\tfrac{1}{2}mb^2) U_1(mb^2, nb)] + \frac{i2}{m} [\sin(\tfrac{1}{2}mb^2) U_1(mb^2, nb) \\ &\quad \left. - \cos(\tfrac{1}{2}mb^2) U_2(mb^2, nb)] \right\}, \quad m = k/\epsilon, \quad n = k\rho_0/z_0. \end{aligned} \tag{22}$$

COMPUTATION

To evaluate the field distribution on the holographic plate, we return to the sampled source in Eq. (4) and evaluate Eq. (5) at sample points $(l\Delta_{x_0}, m\Delta_{y_0})\Delta_{x_0}$ and Δ_{y_0} are the distances between samples in the x_0, y_0 direction in the hologram. Calculations requires the truncation of infinite series. By remaining reasonably close to the image plane the function remains close to the optical axis. Since higher order Bessel functions are nearly zero in this domain the computation errors will be negligible. The meaning of "reasonably close" will be discussed in the next section. A final calculation would involve a summation of all planes in the volume of the form

$$U(l\Delta_{x_0}, m\Delta_{y_0}) = \sum_{n=0}^{k-1} F_{\alpha,n}(l\Delta_{x_0}, m\Delta_{y_0}), \tag{23}$$

where k is the total number of image planes in the data volume, and $F_{\alpha,n}$ is the diffraction pattern of the nth plane. The resulting samples of $U(x_0, y_0)$ can then be encoded by Burch's method, as explained previously.

WHITE LIGHT CHARACTERISTICS

As stated previously, image plane holography shares the characteristic of reconstruction of the wave front in white light. Referring back to Fig. 1, we see that the reference beam strikes the holographic plate at angle θ_r. The object beam is incident at the angle 0°. We can qualitatively say that the purpose of the lens is to localize each object point on the holographic plate. Unlike Fresnel holograms, where each point is recorded over the entire holographic plate, in image plane holography, each point is recorded over an area that is dependent upon

(1) the extent of the focus of the point,
(2) the amount of diffraction caused by the imaging lens.

An image plane hologram cut in half will not reconstruct a full image of the object, as will a Fresnel hologram.

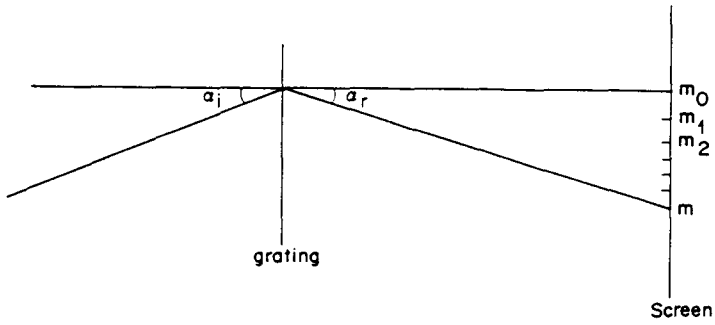

Fig. 3. Light incident on diffraction grating. α_i, angle of incidence; α_r, angle of diffraction; m_0, m_1, ... orders of diffraction.

Viewing a hologram in white light is dependent on the color dispersion of the carrier fringes which form the hologram grating. The blur of an image point a distance R_i from the hologram plane reconstructed by a white light source producing wavelengths from λ to $\lambda + \Delta\lambda$ is given by[7]

$$\Delta x = (R_i \Delta\lambda)\,(d\alpha_r/d\lambda). \tag{24}$$

$d\alpha_r/d\lambda$ is the dispersion of the hologram grating. The grating equation states $d(\sin\alpha_i + \sin\alpha_r) = m\lambda_0$, as apparent in Fig. 3. α_i = angle of incidence of light on the grating, α_r = angle of observation, λ_0 = wavelength of illuminating light, and d = spacing between fringes in the grating,

When the hologram is illuminated by the reference beam at angle $\alpha_i = \theta_r$ the object is reconstructed at $\alpha_r = 0$, giving the relationship

$$m = d \sin\theta_r/\lambda_0. \tag{25}$$

The angular dispersion is found from the grating equation

$$d\alpha_r/d\lambda = m/d\cos\alpha_r. \tag{26}$$

Substituting for m and $\alpha_r = 0$,

$$d\alpha_r/d\lambda = \sin\theta_r/\lambda_0, \tag{27}$$

giving the blur of an image point

$$\Delta x = R_i \sin\theta_r(\Delta\lambda/\lambda). \tag{28}$$

The depth of a scene reproducible by IPH is found[7,12] from the angular spread in the image

$$\theta_{obs} = \Delta x/R_v = R_i D_0/R_v^2, \tag{29}$$

where D_0 is the diameter of the pupil aperture for viewing the hologram. In the case of the eye, $D_0 = 4 \times 10^{-3}$ m. Acceptable blurring is no greater than $\Delta x = 10^{-4}$ m. For a viewing distance $R_v = 1$ m we receive $R_i = 0.025$ m or an overall depth in front and behind the holographic plate of 5 cm.

SUMMARY

We are presently fabricating, optically, a hologram of this sort as an indication of the quality of the image produced. It should be stressed that computer generation allows enhancement

of specific features in the volume space which is an attractive quality, both in medical imaging and in computer assisted design. Together with the white light characteristics, which simplify viewing in such places as operation theaters, this factor has motivated us to investigate algorithms for work in a cellular system such as presented in Ref. 2, which will allow parallel processing of the data base in order to shorten processing time.

REFERENCES

1. Robert J. Perlmutter and Stephen S. Friedland, Computer Graphics and Applications. *IEEE Trans.* **3**, 47 (1983).
2. Howard L. Davidson and Stephen S. Friedland, *Proc. SPIE* **437**, 32–35 (1983).
3. S. A. Benton, *J. Opt. Soc. Am.* **59**, 1454A (1969).
4. J. J. Burch, *Proc. IEEE* **55**, 599 (1967).
5. A. W. Lohmann and B. R. Brown, *IBM J. Res. Develop.* **13**, 160–68 (1969).
6. D. Herbison-Evans, private communication.
7. Gerald B. Brandt, *Appl. Opt.* **8**, 1421 (1969).
8. L. Rosen, *Appl. Phys. Lett.* **9**, 337 (1966).
9. G. W. Stroke, *Phys. Lett.* **23**, 325 (1966).
10. J. W. Goodman, *Introduction to Fourier Optics*. McGraw-Hill, New York (1968).
11. A. Papoulis, *Systems and Transforms with Applications in Optics*. McGraw-Hill, New York (1968).
12. I. S. Klimenko, E. I. Kucheryavenko and G. V. Skrotskii, *Sov. J. Quantum Electron.* **4**, 672 (1974).